Supplemental Methods

Materials

Mice were purchased from Jackson Laboratory (Bar Harbor, ME) and insulin (Novolin R, NDC 0169-1833-11) was from Novo Nordisk (Princeton, NJ). cOmplete protease inhibitor cocktail was from Roche Diagnostics (Indianapolis, IN) and deacetylation inhibitor cocktail was from Santa Cruz Biotechnology (Dallas, TX). Coomassie protein reagent and chemiluminescent western blotting detection system were from Thermo Scientific (Rockford, IL). Antibodies for acetyl-lysine (#9814), COX4 (#4844), phospho-FoxO3a (#9466), and FoxO3a (#2497) were from Cell Signaling Technologies (Danvers, MA); EHHADH (#sc-99386) was from Santa Cruz; GAPDH (58RGM2-65) was from Advanced Immunochemical, Inc. (Long Beach, CA); MitoProfile OXPHOS cocktail (#ab110413) and PDH (#ab110333) were from Abcam (Cambridge, MA); and Vinculin (#CP74) was from EMD Millipore (Billerica, MA). Protein gels were from Bio-Rad Laboratories (Hercules, CA). The AllPrep DNA/RNA/Protein Mini Kit was from Qiagen (Valencia, CA), and the StepOnePlus^{TM} Real-Time PCR System, StepOnePlus^{TM} software and SYBR® Green PCR Master Mix were from Applied Biosystems (Grand Island, NY). U-[$^{13}C_{16}$] potassium palmitate, bovine serum albumin (BSA), and isotope-labeled and unlabeled standards for acyl-CoAs, glycolysis, and TCA cycle intermediates were purchased from Sigma-Aldrich (St. Louis, MO). Isotope-labeled standards for carnitine analysis as well as $^{13}C_6$-$^{15}N_2$ lysine, U-[$^{13}C_6$] glucose and 2,3-[$^{13}C_2$] sodium pyruvate were from Cambridge Isotope Laboratories (Tewksbury, MA). Isotope-labeled (d8) acetyl-lysine was from C/D/N Isotopes Inc. (Pointe-Claire, Quebec, Canada). All mass spectrometry grade solvents were from Sigma-Aldrich.

Mitochondrial Isolation

Renal cortex was rinsed in cold PBS and coarsely chopped on ice containing 10mM PBS-EDTA. Tissue was homogenized in a dounce homogenizer in cold extraction media [250mM sucrose, 25mM KCl, 5mM $MgCl_2$, 10mM Tris, 1mM DTT, 0.2% BSA, and 2 cOmplete Protease Inhibitor Cocktail Tablets (Roche Applied Science, Indianapolis, IN) in water; pH 7.4]. Homogenized samples were centrifuged at 900 x g for 5 minutes at 4^{o}C to pellet nuclei and unbroken cells. Supernatant was transferred and centrifuged at 6200 x g for 10 minutes at 4^{o}C. Pellets were resuspended in extraction media and centrifuged at 6200 x g for 10 minutes at 4^{o}C to separate mitochondrial fraction [modified from (1)].

Mitochondrial Respiration

All measurements of oxygen consumption rates (OCR) were performed in 24 well plates using an XF24 Extracellular Flux Analyzer (Seahorse Bioscience, North Billerica, MA). Plates containing 3 µg of freshly isolated mitochondria per well in MAS buffer (70mM sucrose, 220mM mannitol, 10mM KH_2PO_4, 5mM $MgCl_2$, 2mM HEPES, 1mM EGTA, and 0.2% fatty acid-free BSA, pH 7.2) were centrifuged at 2000 x g for 10 minutes at 4^{o}C prior to initiation of experiments, and either 2mM pyruvate and 2mM malate or 25mM succinate and 10µM rotenone in MAS was added to each well. Substrates provided in sequential order were 10mM ADP, 20µM oligomycin, 40µM carbonyl cyanide p-(triflurомethoxy) phenylhydrazone (FCCP), and 15µl/ml antimycin A. OCR measurements were obtained by the Molecular Phenotyping Core at the University of Michigan.

Immunoprecipitation and Western blot analysis

For determination of protein acetylation, kidney cortex was lysed in RIPA buffer containing protease inhibitor and deacetylation inhibitor cocktails. Total protein was estimated by the Bradford-Lowry method. Total GAPDH, EHHADH or FoxO3a were immunoprecipitated from 60 μg total protein. Proteins were separated on a 4-20% gel and probed with acetylated lysine antibody or phospho-FoxO3a antibody. Gels were stripped and re-probed for total GAPDH, EHHADH, or FoxO3a for normalization. For western blot analysis, isolated mitochondria or kidney cortex were homogenized in RIPA buffer containing protease inhibitors and total protein was estimated by Bradford-Lowry method. Forty μg total protein was separated on a 4-20% protein gel and probed with MitoProfile Total OXPHOS Rodent WB antibody cocktail, Cox4, PDH or acetyl-lysine antibody. Blots were re-probed against vinculin as a loading control. Immunoblots were visualized using Pierce Enhanced Chemiluminescence Western blotting detection system and quantified using NIH Image J (2).

Mitochondrial DNA quantification

Levels of mtDNA were measured by normalizing the mitochondrial gene (cytochrome b) to the nuclear gene (actin) as previously described (3, 4). Briefly, DNA was extracted from kidney cortex of 24-week-old control and diabetic mice (n = 7/group) using AllPrep DNA/RNA/Protein Mini Kit according to the manufacturer's protocol. Real-time PCR amplification and SYBR Green fluorescence detection were performed using the StepOnePlus^{TM} Real-Time PCR System. A total of 2 ng genomic DNA was used for

mtDNA and nuclear DNA markers and 2 µmol/l was used of both forward and reverse gene-specific primers.

Targeted metabolomics analysis by LC/MS and GC/MS

Plasma (20 µl), urine (500 fmol creatinine), renal cortex, mitochondria isolated from renal cortex, and sciatic nerve were subjected to targeted metabolomics analysis by LC/MS and GC/MS for determination of acyl-CoAs, acyl-carnitines, glycolytic and TCA cycle intermediates, and amino acids. For tissue and mitochondrial extracts, metabolite concentrations were normalized to tissue weight or protein content, which was determined by the Bradford-Lowry method. Data extraction and peak area analyses were performed using MassHunter software (Agilent Technologies, New Castle, DE).

Long-chain fatty acyl-CoAs and acyl-carnitines were quantified by LC/ESI/MS/MS as previously described (5, 6). Briefly, samples were homogenized in 25mM phosphate buffer (pH 4.9) and extracted with cold 2:1:1 isopropanol:acetonitrile:methanol. Known amounts of C17:0 acyl-CoA and isotope-labeled carnitines were used as internal standards. For LC/ESI/MS/MS analysis, an Agilent 6410 triple quadruple MS system equipped with an Agilent 1200 LC system and electrospray ionization (ESI) source was utilized. Acyl-CoA and acyl-carnitine species were detected in the multiple reaction monitoring (MRM) mode and relative peak areas were obtained.

Glycolytic and TCA cycle intermediates were extracted and measured as previously described (7, 8). Briefly, samples were kept on ice and sonicated in 8:1:1 methanol:chloroform:water. For measurement of steady state metabolites, isotope-labeled internal standards and norvaline were added prior to extraction. For LC/MS

analysis, an Agilent 6520 high resolution quadruple-time of flight (Q-TOF) instrument coupled to an Agilent 1200 HPLC system with an ESI source was used. For GC/MS analysis (9), extracted metabolites and standards were dried, resuspended in 20 mg/ml methoxyamine hydrochloride in pyridine for 90 minutes at 37^{o}C, and derivatized using N-methyl-N-(tert-butyldimethylsilyl)-trifluoroacetamide (MTBSTFA)+ 1% t-butyl-dimethylchlorosilane (t-BDMCS), heated at 70^{o}C for 30 minutes followed by overnight at room temperature. An Agilent 6890 was used for analysis. For both LC/MS and GC/MS analysis, steady state concentrations were determined by calculating the ratio of each metabolite peak area to that of the closest-matching isotope-labeled standard. Metabolite concentrations were determined using calibration curves generated from known concentrations of authentic standards and equal concentrations of ^{13}C-labeled compounds as were present in the samples. For flux analysis, the percent isotopologue enrichment for each compound was determined. Given the isotopomers used, one turn through the TCA cycle generated metabolites from acetyl-CoA designated as m + 2 (mass + 2) due to the incorporation of two ^{13}C labels. During the second turn of the TCA cycle, citrate was m + 4 with four ^{13}C labels, after which one ^{13}C label was lost as CO_2. Therefore, remaining TCA cycle intermediates were m + 3 after the second turn through the TCA cycle. Pyruvate, an anaplerotic substrate, can also enter the TCA cycle through oxaloacetate. This would contribute three or five ^{13}C labels (m + 3, m + 5) to citrate during condensation with unlabeled or labeled acetyl-CoA, respectively. Both anaplerosis (pyruvate to oxaloacetate) and acetyl-CoA could contribute to m + 3 labeled aspartate. To control for different glucose and palmitate levels between diabetic and control animals, and therefore the different percentage of labeled glucose and palmitate

available, final isotopologue enrichment was corrected for the average plasma concentrations of labeled glucose (m + 6) or labeled palmitate (m + 16).

Amino acids were measured using an Agilent 6890 GC/MS following purification and derivatization of samples using an EZ:faast kit (Phenomenex, Torrance, CA) as previously described (10). ^{13}C-labeled amino acids were used as internal standards.

Protein-bound acetyl-lysine residues were quantified by LC/ESI/MS/MS (11). Briefly, tissue proteins were precipitated with ice-cold 10% trichloroacetic acid and delipidated with water/methanol/water-saturated diethyl ether (1:3:7; vol/vol/vol). Known amounts of isotope-labeled internal standards were added. The precipitated proteins were hydrolyzed overnight at 110°C in 6N hydrochloric acid, dried and dissolved in 50% methanol. For LC/ESI/MS/MS analysis, an Agilent 6410 triple quadruple MS system equipped with an Agilent 1200 LC system and ESI source was operated in positive ion mode. Acetyl-lysine, lysine, and the isotope-labeled standards were detected in MRM mode and relative peak areas were obtained.

As a technical control, pooled samples were regularly interspersed and analyzed by both LC-MS and GC/MS to determine the reproducibility of quantification with time. For LC/MS, a CV < 20% was considered acceptable while for GC/MS, a CV < 10% was allowed.

Pathway Analysis

To visualize genomic and metabolomic data together, we utilized the Cytoscape (http://www.cytoscape.org/) plugin Metscape (12). A significance cutoff of $p < 0.05$ (metabolites) or $q < 0.05$ (genes) was used.

Supplemental References

1. Frezza C, Cipolat S, and Scorrano L. Organelle isolation: functional mitochondria from mouse liver, muscle and cultured fibroblasts. *Nature protocols.* 2007;2(2):287-95.
2. Rasband WS. Bethesda, MD: U.S. National Institutes of Health; 1997-2015.
3. Vincent AM, Edwards JL, McLean LL, Hong Y, Cerri F, Lopez I, Quattrini A, and Feldman EL. Mitochondrial biogenesis and fission in axons in cell culture and animal models of diabetic neuropathy. *Acta neuropathologica.* 2010;120(4):477-89.
4. Edwards JL, Quattrini A, Lentz SI, Figueroa-Romero C, Cerri F, Backus C, Hong Y, and Feldman EL. Diabetes regulates mitochondrial biogenesis and fission in mouse neurons. *Diabetologia.* 2010;53(1):160-9.
5. Golej DL, Askari B, Kramer F, Barnhart S, Vivekanandan-Giri A, Pennathur S, and Bornfeldt KE. Long-chain acyl-CoA synthetase 4 modulates prostaglandin E(2) release from human arterial smooth muscle cells. *Journal of lipid research.* 2011;52(4):782-93.
6. Han CY, Umemoto T, Omer M, Den Hartigh LJ, Chiba T, LeBoeuf R, Buller CL, Sweet IR, Pennathur S, Abel ED, et al. NADPH oxidase-derived reactive oxygen species increases expression of monocyte chemotactic factor genes in cultured adipocytes. *The Journal of biological chemistry.* 2012;287(13):10379-93.
7. Hinder LM, Vivekanandan-Giri A, McLean LL, Pennathur S, and Feldman EL. Decreased glycolytic and tricarboxylic acid cycle intermediates coincide with

peripheral nervous system oxidative stress in a murine model of type 2 diabetes. *The Journal of endocrinology.* 2013;216(1):1-11.

8. Lorenz MA, El Azzouny MA, Kennedy RT, and Burant CF. Metabolome response to glucose in the beta-cell line INS-1 832/13. *The Journal of biological chemistry.* 2013;288(15):10923-35.
9. Mamer O, Gravel SP, Choiniere L, Chenard V, St-Pierre J, and Avizonis D. The complete targeted profile of the organic acid intermediates of the citric acid cycle using a single stable isotope dilution analysis, sodium borodeuteride reduction and selected ion monitoring GC/MS. *Metabolomics : Official journal of the Metabolomic Society.* 2013;9(1019-30.
10. Kugler F, Graneis S, Schreiter PP, Stintzing FC, and Carle R. Determination of free amino compounds in betalainic fruits and vegetables by gas chromatography with flame ionization and mass spectrometric detection. *Journal of agricultural and food chemistry.* 2006;54(12):4311-8.
11. Tareke E, Forslund A, Lindh CH, Fahlgren C, and Ostman E. Isotope dilution ESI-LC-MS/MS for quantification of free and total Nepsilon-(1-Carboxymethyl)-L-Lysine and free Nepsilon-(1-Carboxyethyl)-L-Lysine: comparison of total Nepsilon-(1-Carboxymethyl)-L-Lysine levels measured with new method to ELISA assay in gruel samples. *Food chemistry.* 2013;141(4):4253-9.
12. Karnovsky A, Weymouth T, Hull T, Tarcea VG, Scardoni G, Laudanna C, Sartor MA, Stringer KA, Jagadish HV, Burant C, et al. Metscape 2 bioinformatics tool for the analysis and visualization of metabolomics and gene expression data. *Bioinformatics.* 2012;28(3):373-80.

Supplemental Table 1: Mouse kidney cortex mRNA expression of genes in glycolysis, fatty acid metabolism, and the TCA cycle

Pathway	Gene Name	Gene Symbol	Log2 Fold Change	q-value
Glycolysis	Pyruvate kinase liver and red blood cell	***Pklr***	**0.84**	**0**
	Pyruvate kinase muscle	***Pkm2***	**0.65**	**0**
	Phosphoenolpyruvate carboxykinase 2 mitochondrial	***Pck2***	**0.6**	**0**
	Lactate Dehydrogenase D	***Ldhd***	**-0.73**	**0**
	Hexokinase 1	***Hk1***	**0.62**	**0.01**
	Phosphofructokinase liver	***Pfkl***	**0.19**	**0.09**
	Enolase 2 gamma neuronal	*Eno2*	0.98	0.22
	Phosphofructokinase platelet	*Pfkp*	0.76	0.24
	Phosphoenolpyruvate carboxykinase cytosolic	*Pck1*	0.27	0.26
	Triose phosphate isomerase	*Tpi1*	-0.04	0.39
	phosphofructokinase muscle	*Pfkm*	-0.02	0.46
	Fructose bisphosphate aldolase B	*Aldob*	-0.01	0.49
	Hexokinase 3	*Hk3*	2.05	> 0.50
	Phosphoglucose isomerase	*Gpi1*	0.03	> 0.50
	Fructose bisphosphate aldolase A	*Aldoa*	0.03	> 0.50
	Enolase 3 beta muscle	*Eno3*	0.11	> 0.50
	Phosphoglycerate mutase 2	*Pgam2*	0.38	> 0.50
	Lactase Dehydrogenase B	*Ldhb*	0.01	> 0.50
	Pyruvate carboxylase	*Pcx*	0.04	> 0.50
	Hexokinase 2	*Hk2*	N/A	
	Glyceraldehyde 3-phosphate dehydrogenase	*Gapdh*	N/A	
	Phosphoglycerate kinase	*Pgk1*	N/A	
	Phosphoglycerate mutase 1	*Pgam1*	N/A	
	Enolase 1 non-neuronal	*Eno1*	N/A	
	Lactase Dehydrogenase A	*Ldha*	N/A	
	Lactase Dehydrogenase C	*Ldhc*	N/A	
Fatty acid metabolism	Fatty acid synthase	***Fasn***	**-0.57**	**0.01**
	Enoyl-Coenzyme A, hydratase/3-hydroxyacyl Coenzyme A dehydrogenase	***Ehhadh***	**-0.17**	**0.02**
	Enoyl-Coenzyme A delta isomerase 1	***Eci1***	**0.27**	**0.04**
	Acetyl-Coenzyme A acetyltransferase 1	***Acat1***	**-0.27**	**0.07**
	Catalase	*Cat*	-0.14	0.25
	Methylmalonyl-Coenzyme A mutase	*Mut*	-0.16	0.26

Pathway	Gene Name	Gene Symbol	Log2 Fold Change	q-value
Fatty acid metabolism	Carnitine palmitoyltransferase 1c	*Cpt1c*	0.26	0.43
	Hydroxyacyl-Coenzyme A dehydrogenase	*Hadh*	-0.02	0.49
	Carnitine palmitoyltransferase 1a	*Cpt1a*	0.11	> 0.50
	Acetyl-Coenzyme A carboxylase alpha	*Acaca*	N/A	
	Acyl-CoA synthetase	*Acss2*	N/A	
TCA cycle	Isocitrate dehydrogenase NAD+ beta	*Idh3b*	-0.11	0.26
	Alpha-ketoglutarate dehydrogenase lipoamide	*Ogdh*	-0.16	0.27
	Isocitrate dehydrogenase NAD+ gamma	*Idh3g*	-0.08	0.29
	Pyruvate dehydrogenase E1 alpha 1	*Pdha1*	-0.07	0.33
	Pyruvate dehydrogenase lipoamide beta	*Pdhb*	-0.08	0.35
	Bckdha branched chain ketoacid dehydrogenase E1, alpha polypeptide	*Bckdha*	-0.14	0.36
	Bckdha branched chain ketoacid dehydrogenase E1, beta polypeptide	*Bckdhb*	-0.14	0.36
	Isocitrate dehydrogenase NAD+ alpha	*Idh3a*	-0.12	0.37
	Succinate dehydrogenase complex, subunit C	*Sdhc*	-0.06	0.39
	Succinate dehydrogenase complex, subunit A, flavoprotein (Fp)	*Sdha*	-0.05	0.39
	Isocitrate dehydrogenase NADP+ soluble	*Idh1*	-0.04	0.41
	Citrate synthase	*Cs*	-0.04	0.43
	Dlat dihydrolipamide S-acetyltransferase (E2 componenet of pyruvate dehydrogenase complex)	*Dlat*	-0.05	0.44
	Isocitrate dehydrogenase NADP+ mitochondrial	*Idh2*	-0.05	0.44
	Bckdk branched cain ketoacid dehydrogenase kinase	*Bckdk*	-0.07	0.44
	Dlst dihydrolipoamide S-succinyltransferase (E2 component of 2-oxoglutarate complex)	*Dlst*	-0.04	0.44
	Malate dehydrogenase 2, NAD (mitochondrial)	*Mdh2*	-0.03	0.44
	Fumarate hydratase 1	*Fh1*	-0.04	0.45
	Glutamate decarboxylase 1	*Gad1*	0.26	0.46
	Aconitase mitochondrial	*Aco2*	-0.03	0.46
	Succinate-Coenzyme A ligase, GDP-forming, beta subunit	*Suclg2*	-0.02	0.49

Pathway	Gene Name	Gene Symbol	Log2 Fold Change	q-value
TCA cycle	Succinate dehydrogenase complex, subunit B, iron sulfur (Ip)	*Sdhb*	-0.02	0.49
	Aconitase	*Aco1*	-0.02	> 0.50
	Succinate dehydrogenase complex, subunit D	*Sdhd*	-0.01	> 0.50
	Malate dehydrogenase 1, NAD (soluble)	*Mdh1*	0.01	> 0.50
	Malate dehydrogenase 1B, NAD (soluble)	*Mdh1b*	0.07	> 0.50
	Pyruvate dehydrogenase E1 alpha 2	*Pdha2*	N/A	
	Succinate-Coenzyme A ligase, ADP-forming, beta subunit	*Sucla2*	N/A	

N/A = not on the array. Log2 Fold Change is *db/db* versus *db/+*. Significance was defined as FDR < 0.1 using the entire array.

Supplemental Table 2: Targeted metabolomic analysis of kidney cortex from control and diabetic mice

Metabolite	12 week		24 week	
	Log Fold Change	p value	Log Fold Change	p value
Hexose 6-phosphates	**0.6364**	**0.0299**	0.4044	0.2527
Fructose 1,6-bisphosphate	**0.5642**	**0.0055**	-0.0294	0.9708
Glyceraldehyde 3-phosphate	0.6596	0.4237	**3.3888**	**0.0044**
2,3 Phosphoglycerate	0.0281	0.9156	**1.3133**	**0.0218**
Phosphoenolpyruvate	0.7157	0.2057	**0.9539**	**0.0008**
Pyruvate	0.0290	0.4757	**0.6430**	**0.0034**
Lactate	**1.3945**	**0.0152**	**0.7886**	**0.0178**
Acetyl CoA	0.4010	0.0739	ND	
Citrate	0.5053	0.0638	1.3406	0.1388
α-Ketoglutarate	0.2016	0.4314	ND	
Succinate	0.2892	0.1744	-0.0101	0.9799
Fumarate	**0.6891**	**0.0257**	**1.5259**	**0.0001**
Malate	**1.1650**	**0.0007**	**1.1206**	**0.0005**
Oxaloacetate	ND		**0.7121**	**0.0177**
Ribulose/Xylulose 5-phosphates	0.6049	0.1417	-1.3108	0.0901
Sedoheptulose 7-phosphate	**0.8996**	**0.0245**	-0.8884	0.3235
AMP/ATP	ND		-2.6439	0.1863
ADP/ATP	ND		-0.3003	0.3908
Acetylcarnitine (C2)	0.5553	0.0555	**2.5083**	**0.0219**
Propionylcarnitine (C3)	**1.0598**	**<0.0001**	**2.7290**	**0.0024**
Butyrylcarnitine (C4)	**1.9482**	**<0.0001**	**2.2790**	**0.0002**
Isovalerylcarnitine (C5)	**1.0969**	**0.0021**	**3.0256**	**0.0008**
Hexanoylcarnitine (C6)	**1.2216**	**<0.0001**	**1.4696**	**0.0087**
Octanoylcarnitine (C8)	**0.8681**	**<0.0001**	0.8085	0.1504
Myristoylcarnitine (C14)	**0.6288**	**0.0416**	0.7293	0.2287
Palmitoylcarnitine (C16)	**0.7738**	**0.0001**	**1.1906**	**0.0426**
Alanine	**-0.7651**	**0.0152**	-0.3785	0.1427
Asparagine	-0.3589	0.4745	-0.2901	0.2122
Aspartate	-0.5280	0.1751	-0.4875	0.1839
Cysteine	**-1.9093**	**0.0116**	**-1.2779**	**0.0063**
Glutamate	-0.5319	0.2888	**-0.9539**	**0.0059**
Glutamine	0.4253	0.3825	ND	
Glycine	**-0.9244**	**0.0176**	**-0.9209**	**0.001**

Metabolite	12 week		24 week	
	Log Fold Change	**p value**	**Log Fold Change**	**p value**
Histidine	0.2790	0.5115	-0.5687	0.1227
4-Hydroxyproline	-1.4078	0.0761	-0.8471	0.1277
Isoleucine	0.2605	0.2007	0.3760	0.0974
Leucine	0.0654	0.8091	0.2484	0.2522
Lysine	**-3.1046**	**0.0471**	**-1.9334**	**0.0404**
Methionine	**-0.9481**	**0.0413**	0.3648	0.2103
Ornithine	**-2.0453**	**0.0041**	ND	
Phenylalanine	0.1701	0.7951	-0.0587	0.8302
Proline	-0.3476	0.2984	-0.3229	0.1994
Serine	0.2462	0.7355	**-0.4894**	**0.0237**
Threonine	-0.2359	0.8655	**-0.6799**	**0.0294**
Tryptophan	-0.5320	0.2669	**-0.7973**	**0.0232**
Tyrosine	**-0.8605**	**0.0064**	-0.5338	0.0910
Valine	0.2445	0.3984	0.1883	0.4567

ND = not detected above noise. Log fold change is *db/db* versus *db/+*. Significance was defined as $p < 0.05$.

Supplemental Table 3: Targeted metabolomic analysis of mitochondria isolated from kidney cortex from control and diabetic mice

	12 week		24 week	
Metabolite	**Log Fold Change**	**p value**	**Log Fold Change**	**p value**
Pyruvate	0.1977	0.6264	**2.6539**	**0.0037**
Lactate	-0.3827	0.22	**2.5431**	**0.0002**
Acetyl CoA	0.369	0.3719	ND	
Citrate	-0.2527	0.5937	**1.4481**	**0.0042**
α-Ketoglutarate	**0.9036**	**0.0137**	1.5535	0.0917
Succinate	0.1036	0.7668	**1.9204**	**0.0035**
Fumarate	0.817	0.2098	1.5126	0.2839
Malate	0.8111	0.1151	1.5494	0.3545
Oxaloacetate	-0.1734	0.7966	0.862	0.2015
Acetylcarnitine (C2)	**1.5902**	**0.0048**	**3.6093**	**0.0032**
Propionylcarnitine (C3)	**1.4401**	**0.0027**	**3.506**	**0.0008**
Butyrylcarnitine (C4)	**1.4383**	**0.0003**	**2.6377**	**0.0006**
Isovalerylcarnitine (C5)	0.0587	0.9284	**3.0256**	**0.0008**
Hexanoylcarnitine (C6)	0.6453	0.4142	**2.0206**	**0.0008**
Octanoylcarnitine (C8)	0.1255	0.6571	**1.43**	**0.0126**
Myristoylcarnitine (C14)	0.2137	0.7236	**1.4784**	**0.0015**
Palmitoylcarnitine (C16)	0.4265	0.329	**1.8618**	**0.0008**
Octanoylcarnitine (C8): Palmitoylcarnitine (C16)	0.9101	0.7645	0.2254	0.0715

ND = not detected above noise. Log fold change is *db/db* versus *db/+*. Significance was defined as $p < 0.05$.

Supplemental Table 4: Metabolic flux analysis kidney cortex, sciatic nerve and retina from 24-week-old control and diabetic mice.

	$^{13}C_6$-Glucose					
	Kidney		**Nerve**		**Retina**	
	Fold Change	**p value**	**Fold Change**	**p value**	**Fold Change**	**p value**
Hexose 6-phosphates m+6	**3.0988**	**0.0104**	0.6806	0.3503	0.9421	0.8725
2, 3 Phosphoglycerates m+3	**3.6026**	**0.0448**	1.392	0.1678	ND	
Phosphoenolpyruvate m+3	**5.321**	**0.0276**	1.0816	0.8472	**2.5775**	**0.0221**
Lactate m+2						
Lactate m+3	**3.8155**	**0.0003**	**2.1025**	**0.0018**	**4.8863**	**0.0001**
Ribulose/Xylulose 5-phosphates m+3	**0.284**	**0.0012**	ND		1.1691	0.369
Ribulose/Xylulose 5-phosphates m+5	1.1739	0.6414	ND		1.65	0.4222
Sedoheptulose 7-phosphate m+3	**0.252**	**0.0177**	ND		ND	
Sedoheptulose 7-phosphate m+5	**0.1847**	**0.0008**	ND		ND	
Acetyl-CoA m+2	**8.5419**	**0.0023**	ND		ND	
Citrate m+2	**2.1495**	**0.0009**	0.8431	0.1951	**2.2467**	**0.0006**
Citrate m+3	1.6353	0.3294	0.6663	0.1983	2.7153	0.1548
Citrate m+4	**2.9553**	**0.0132**	0.9702	0.9138	**5.0973**	**0.0044**
Citrate m+5	**2.0093**	**0.0158**	**0.3154**	**0.0064**	3.6281	0.138
Citrate m+6	1.3018	0.6589	**0.5816**	**0.0024**	3.634	0.3395
Glutamate m+2	**1.8845**	**0.0008**	0.586	0.0706	**2.1869**	**0.0048**
Glutamate m+3	**1.7162**	**0.0106**	0.6023	0.1443	2.8976	0.1164
Glutamate m+4	**4.6399**	**0.0064**	0.9377	0.8466	**7.729**	**0.0231**
Glutamate m+5	**2.7677**	**0.0247**	0.1535	0.2707	ND	
Succinate m+2	ND		ND		ND	
Succinate m+3	ND		ND		ND	
Succinate m+4	**1.9596**	**0.0329**	ND		ND	
Malate m+2	**1.5679**	**<0.0001**	1.0056	0.8671	**2.0597**	**0.0015**
Malate m+3	**1.8326**	**0.0003**	0.7677	0.457	2.7907	0.1107
Malate m+4	1.6834	0.3095	1.348	0.1974	**4.1516**	**0.0197**
Aspartate m+2	**1.9881**	**0.0003**	ND		**2.4134**	**0.0219**
Aspartate m+3	**1.4638**	**0.0183**	ND		ND	
Aspartate m+4	ND		ND		ND	

Supplemental Table 4: Metabolic flux analysis kidney cortex, sciatic nerve and retina from 24-week-old control and diabetic mice.

	$^{13}C_6$-Glucose					
	Kidney		**Nerve**		**Retina**	
	Fold Change	**p value**	**Fold Change**	**p value**	**Fold Change**	**p value**
Palmitate m+16						
Acetylcarnitine (C2) m+2						
Propionylcarnitine (C3) m+3						
Butyrylcarnitine (C4) m+4						
Isovalerylcarnitine (C5) m+5						
Hexanoylcarnitine (C6) m+6						
Octanoylcarnitine (C8) m+8						
Myristoylcarnitine (C14) m+14						
Palmitoylcarnitine (C16) m+16						

ND = not detected above noise. Fold change is db/db vs db/+. Significance was defined as $p < 0.05$.

Supplemental Table 4: Metabolic flux analysis kidney cortex, sciatic nerve and retina from 24-week-old control and diabetic mice.

	2,3-$^{13}C_2$-Na Pyruvate					
	Kidney		Nerve		Retina	
	Fold Change	p value	Fold Change	p value	Fold Change	p value
Hexose 6-phosphates m+6						
2, 3 Phosphoglycerates m+3						
Phosphoenolpyruvate m+3						
Lactate m+2	**4.8465**	**0.0051**	**2.5721**	**0.0051**	**3.9967**	**0.0002**
Lactate m+3						
Ribulose/Xylulose 5-phosphates m+3						
Ribulose/Xylulose 5-phosphates m+5						
Sedoheptulose 7-phosphate m+3						
Sedoheptulose 7-phosphate m+5						
Acetyl-CoA m+2	**2.2378**	**0.0122**	ND		0.7546	0.5006
Citrate m+2	**2.2192**	**<0.0001**	**1.7644**	**<0.0001**	**2.6773**	**<0.0001**
Citrate m+3	**3.1733**	**0.0003**	**2.4695**	**<0.0001**	**4.9784**	**<0.0001**
Citrate m+4	**2.5997**	**<0.0001**	**1.8235**	**0.0114**	**5.9002**	**0.0013**
Citrate m+5	**2.7148**	**0.0009**	**2.7273**	**<0.0001**	**4.0955**	**0.0002**
Citrate m+6	**1.8152**	**0.001**	**2.2336**	**0.0266**	2.0403	0.3227
Glutamate m+2	**4.5496**	**<0.0001**	**4.9904**	**0.0058**	**4.4431**	**<0.0001**
Glutamate m+3	**6.1519**	**0.0003**	**2.2304**	**0.0005**	**8.6996**	**<0.0001**
Glutamate m+4	**6.3048**	**0.0008**	**2.8205**	**0.0008**	**8.041**	**<0.0001**
Glutamate m+5	**5.3493**	**0.001**	0.937	0.8443	**3.5157**	**0.0087**
Succinate m+2	ND		ND		ND	
Succinate m+3	**2.7855**	**0.0013**	ND		ND	
Succinate m+4	**6.9104**	**0.005**	ND		ND	
Malate m+2	**3.1634**	**0.0002**	**2.1003**	**0.0002**	**2.3816**	**<0.0001**
Malate m+3	**4.0142**	**0.0014**	**3.712**	**<0.0001**	**5.8582**	**<0.0001**
Malate m+4	**5.3064**	**0.0051**	**2.2634**	**0.0011**	1.4175	0.1788
Aspartate m+2	**1.9881**	**0.0003**	ND		**2.4134**	**0.0219**
Aspartate m+3	**1.4638**	**0.0183**	ND		ND	
Aspartate m+4	1.1331	0.6874	ND		ND	

Supplemental Table 4: Metabolic flux analysis kidney cortex, sciatic nerve and retina from 24-week-old control and diabetic mice.

	2,3-$^{13}C_2$-Na Pyruvate					
	Kidney		Nerve		Retina	
	Fold Change	p value	Fold Change	p value	Fold Change	p value
Palmitate m+16						
Acetylcarnitine (C2) m+2						
Propionylcarnitine (C3) m+3						
Butyrylcarnitine (C4) m+4						
Isovalerylcarnitine (C5) m+5						
Hexanoylcarnitine (C6) m+6						
Octanoylcarnitine (C8) m+8						
Myristoylcarnitine (C14) m+14						
Palmitoylcarnitine (C16) m+16						

ND = not detected above noise. Fold

Supplemental Table 4: Metabolic flux analysis kidney cortex, sciatic nerve and retina from 24-week-old control and diabetic mice.

	$^{13}C_{16}$-K Palmitate					
	Kidney		**Nerve**		**Retina**	
	Fold Change	**p value**	**Fold Change**	**p value**	**Fold Change**	**p value**
Hexose 6-phosphates m+6						
2, 3 Phosphoglycerates m+3						
Phosphoenolpyruvate m+3						
Lactate m+2						
Lactate m+3						
Ribulose/Xylulose 5-phosphates m+3						
Ribulose/Xylulose 5-phosphates m+5						
Sedoheptulose 7-phosphate m+3						
Sedoheptulose 7-phosphate m+5						
Acetyl-CoA m+2	0.7762	0.055	ND		0.836	0.6037
Citrate m+2	**3.061**	**0.0381**	**2.4766**	**0.0028**	**2.4106**	**0.0012**
Citrate m+3	0.9083	0.7595	**2.2189**	**0.0073**	**2.0316**	**0.0203**
Citrate m+4	1.0078	0.9865	1.3322	0.3455	1.9244	0.1597
Citrate m+5	1.1682	0.736	0.8948	0.8442	7.4199	0.2069
Citrate m+6	0.5288	0.0629	0.7257	0.1316	1.2128	0.7145
Glutamate m+2						
Glutamate m+3						
Glutamate m+4						
Glutamate m+5						
Succinate m+2	**7.2542**	**0.0384**	**0.2055**	**0.0432**	0.9417	0.9469
Succinate m+3	**3.8196**	**0.0133**	**0.1057**	**0.0012**	**0.1271**	**0.0025**
Succinate m+4	1.2739	0.5007	0.6774	0.4341	1.1724	0.8704
Malate m+2	**1.9734**	**0.0473**	**1.938**	**0.0071**	1.6063	0.5644
Malate m+3	**1.98**	**0.026**	1.6091	0.0859	1.221	0.2771
Malate m+4	2.4056	0.1347	1.7792	0.1131	1.6273	0.383
Aspartate m+2						
Aspartate m+3						
Aspartate m+4						

Supplemental Table 4: Metabolic flux analysis kidney cortex, sciatic nerve and retina from 24-week-old control and diabetic mice.

	$^{13}C_{16}$-K Palmitate					
	Kidney		**Nerve**		**Retina**	
	Fold Change	**p value**	**Fold Change**	**p value**	**Fold Change**	**p value**
Palmitate m+16	**2.0615**	**0.0056**	**2.1389**	**0.0033**	**2.3908**	**0.0196**
Acetylcarnitine (C2) m+2	ND		ND		ND	
Propionylcarnitine (C3) m+3	ND		ND		ND	
Butyrylcarnitine (C4) m+4	2.54	0.0773	**1.947**	**0.0359**	**2.948**	**0.0124**
Isovalerylcarnitine (C5) m+5	0.4381	0.1709	ND		ND	
Hexanoylcarnitine (C6) m+6	1.4311	0.2952	**2.7512**	**0.0141**	1.3437	0.3103
Octanoylcarnitine (C8) m+8	1.6294	0.098	**2.696**	**0.0094**	1.3148	0.3283
Myristoylcarnitine (C14) m+14	**2.1379**	**0.0053**	**2.363**	**0.0011**	**2.3083**	**0.0021**
Palmitoylcarnitine (C16) m+16	**2.1949**	**0.0005**	**2.526**	**0.0011**	**2.7796**	**0.0007**

ND = not detected above noise. Fold change is db/db vs db/+. Significance was defined as $p < 0.05$.

Supplemental Table 5: Pathway summary of In vivo metabolic flux analysis in kidney cortex, sciatic nerve and retina from 24-week-old diabetic mice compared to control mice

Tissue	Isotope-Labeled Substrate	Glycolysis	Pentose Phosphate Pathway	Acyl-carnitines	TCA Cycle
Kidney	$^{13}C_6$-glucose	↑↑	↓		↑↑
	2,3-$^{13}C_2$-Na pyruvate				↑↑
	$^{13}C_{16}$-palmitate			↑	↑↑
Nerve	$^{13}C_6$-glucose	=	ND		↓
	2,3-$^{13}C_2$-Na pyruvate				↑↑
	$^{13}C_{16}$-palmitate			↑↑	↑↓
Retina	$^{13}C_6$-glucose	↑	=		↑
	2,3-$^{13}C_2$-Na pyruvate				↑↑
	$^{13}C_{16}$-palmitate			↑	↑↓

Arrows denote change in flux throughout all (↑↑) or part (↑) of a pathway. Pathways could also be unchanged (=) or exhibit a mixed response (↑↓), in which label incorporation was increased and decreased into individual metabolites in a pathway. ND = not detected above noise. Summary of Fig 5, Suppl Fig 3B, and Suppl Table 4.

Supplemental Figure 1: Transcriptomic analysis of kidney cortex from 24-week-old control and diabetic mice

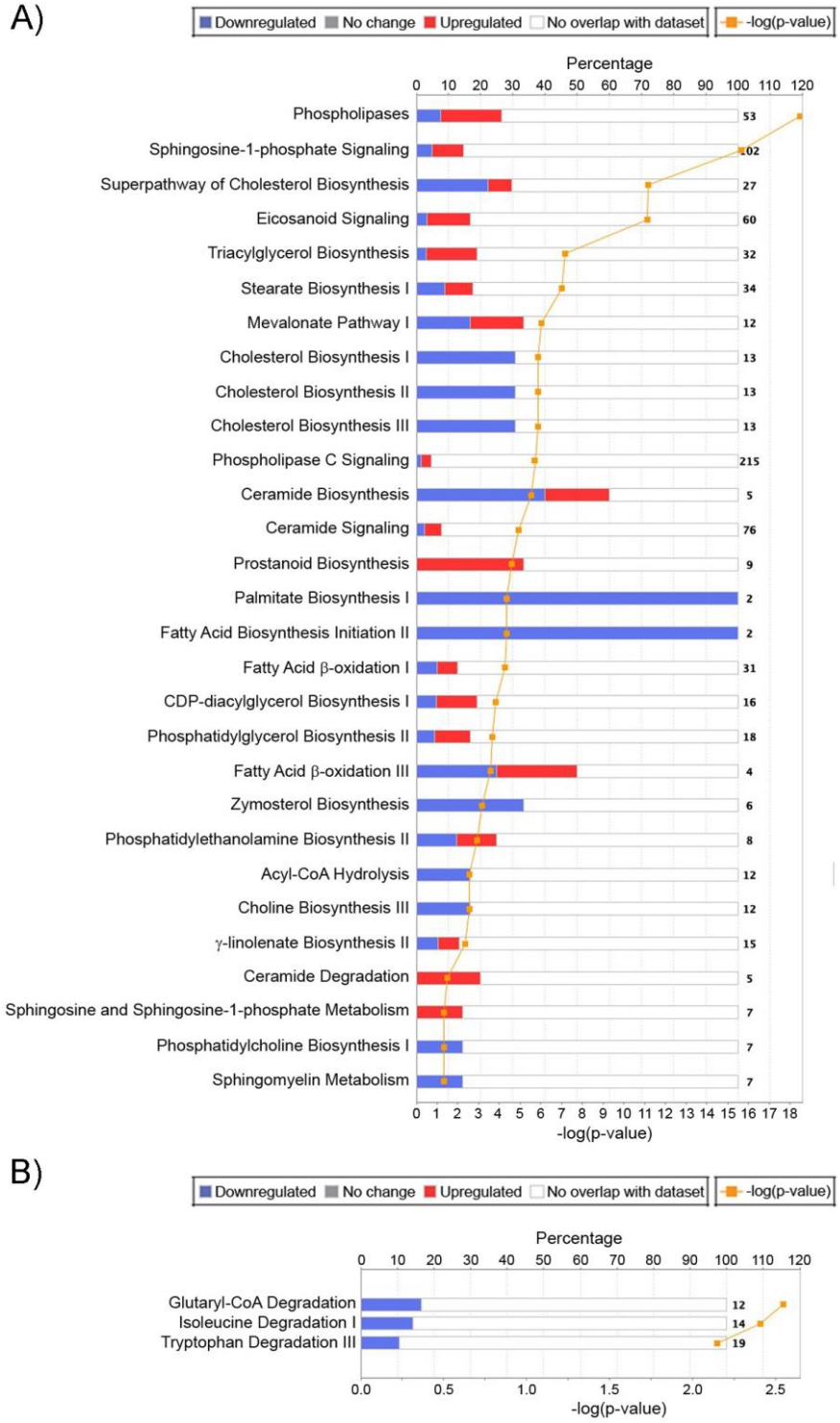

Predicted alteration of pathways involved in (A) lipid metabolism and (B) amino acid metabolism in diabetic versus control mice, with the percentage of genes significantly upregulated (red) and downregulated (blue) (p , 0.05 [-log(p-value) > 1.3], n = 5/group). The number of transcripts in each pathway is shown at the right margin corresponding to each pathway.

Supplemental Figure 2: Transcriptomic and metabolomic analyses of sciatic nerve from 24-week-old control and diabetic mice

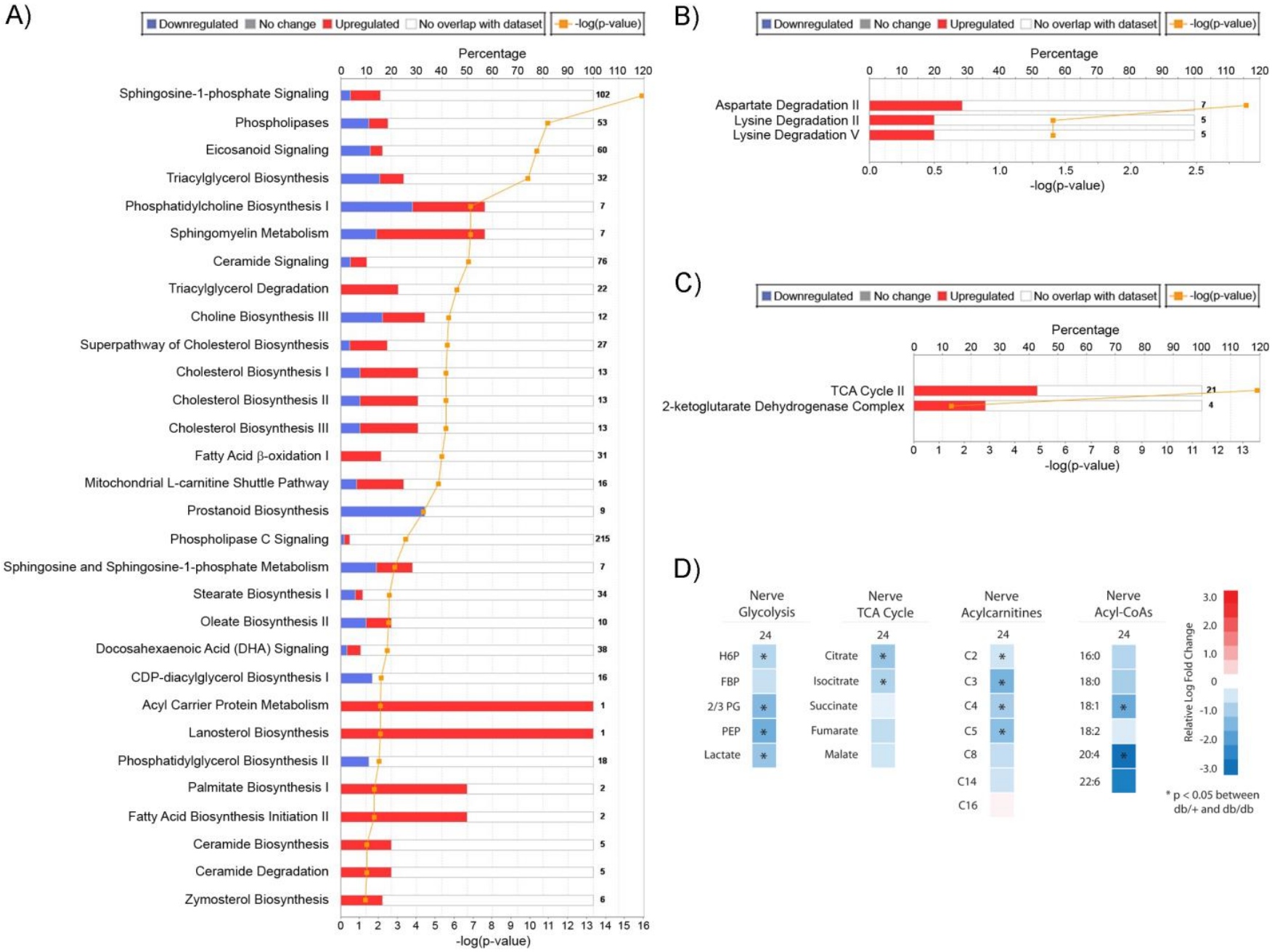

(A-C) Predicted alteration of pathways involved in (A) lipid metabolism, (B) amino acid metabolism and (C) TCA cycle metabolism in diabetic versus control mice with percentage of genes significantly upregulated (red) and downregulated (blue) ($p < 0.05$ [-log(p-value) > 1.3], control n = 9, diabetic n = 10). The number of transcripts in each pathway is shown at the right margin corresponding to each pathway. (D) Relative levels of acylcarnitines and long-chain acyl-CoAs in the sciatic nerve from 24-week-old diabetic versus control mice were depicted as upregulated (red) or downregulated (blue) in diabetic mice (* $p < 0.05$, n = 6/group). Metabolites in glycolysis and the TCA cycle (n = 9/group) are similarly shown for comparative purposes [7]. Both metabolites involved in glucose and fat metabolism were significantly decreased in the sciatic nerve. (* $p < 0.05$).

Supplemental Figure 3: In vivo metabolic flux analysis of 2,3-$^{13}C_2$-Na pyruvate

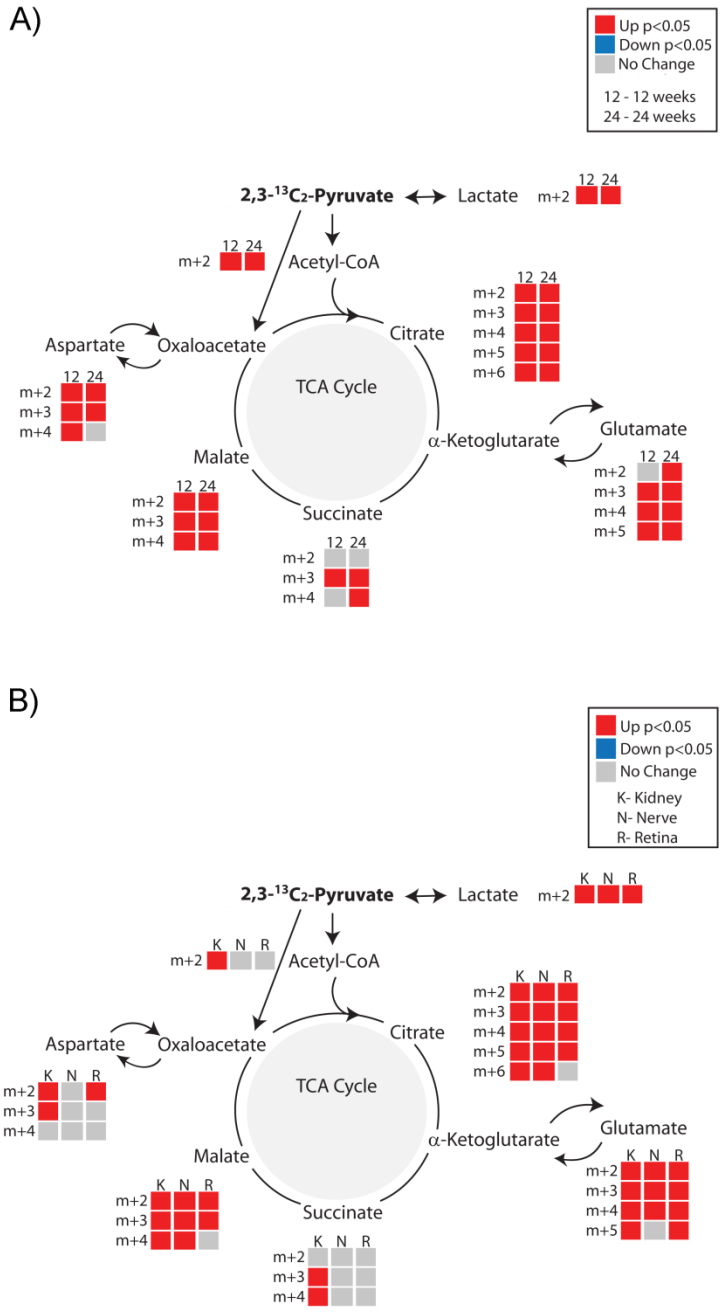

Metabolic flux was determined following administration of 2,3-$^{13}C_2$-Na pyruvate (n = 8/group). (A) Metabolites in the diabetic kidney cortex from 12-week-old and 24-week-old mice or (B) metabolites in diabetic kidney cortex (K), sciatic nerve (N) and retina (R) were depicted as up-regulated (red), down-regulated (blue) or unchanged (gray) compared to control tissues ($p < 0.05$). Upon entry into the TCA cycle through acetyl-CoA, each TCA cycle metabolite incorporates two ^{13}C labels (m+2). Metabolites resulting from a second turn of the TCA cycle would incorporate 2 (citrate, m+4) or 1 (all other intermediates, m+3) additional ^{13}C labels. If labeled pyruvate enters the TCA cycle through oxaloacetate, it will contribute 3 or 5 ^{13}C labels (m+3 or m+5) to citrate during condensation with unlabeled or labeled acetyl-CoA, respectively.

Supplemental Figure 4: Mitochondrial protein acetylation and expression from kidney cortex of 24-week-old control and diabetic mice

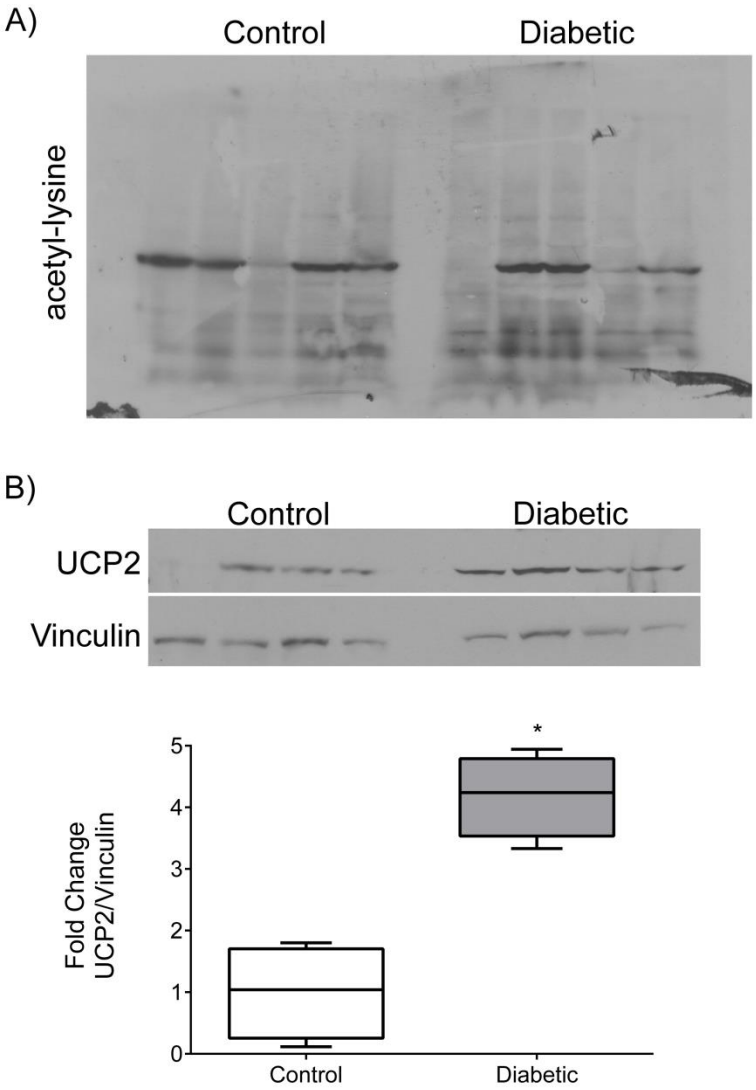

(A) Total lysine acetylation was determined by Western blot of mitochondria isolated from kidney cortex from 24-week-old control (*db/+*) and diabetic (*db/db*) mice (n = 5/group). There was no significant difference in the amount of total acetylation. (B) Protein expression of mitochondrial uncoupling protein 2 (UCP2) was determined by Western blot and normalized to vinculin (n = 4). * $p < 0.05$ using student's two-tailed t-test.

Supplemental Figure 5: Transcriptomic analysis of kidney tubules from diabetic and control subjects

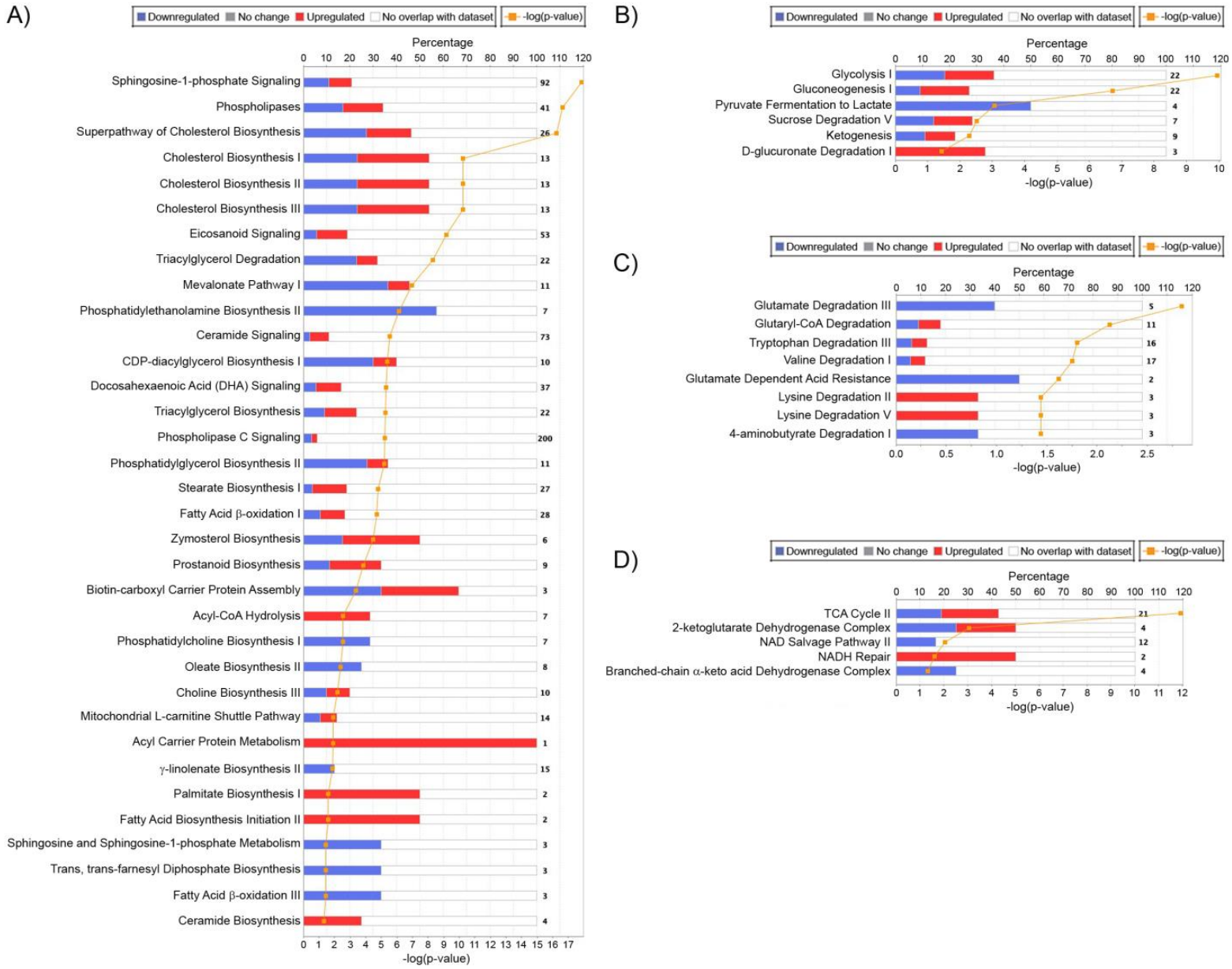

(A-D) Predicted alteration of pathways involved in (A) lipid metabolism, (B) glycolysis, (C) amino acid metabolism and (D) TCA cycle and associated cofactor metabolism in diabetic subjects (Southwestern American Indian cohort, n = 49) versus non-diabetic healthy living donors (n = 32) with the percentage of genes significantly upregulated (red) and downregulated (blue) ($p < 0.05$ [-log(p-value) > 1.3]). The number of transcripts in each pathway is shown to the right of each pathway.

Supplemental Figure 6: MetScape analysis of human kidney tubule transcriptome and urinary metabolites

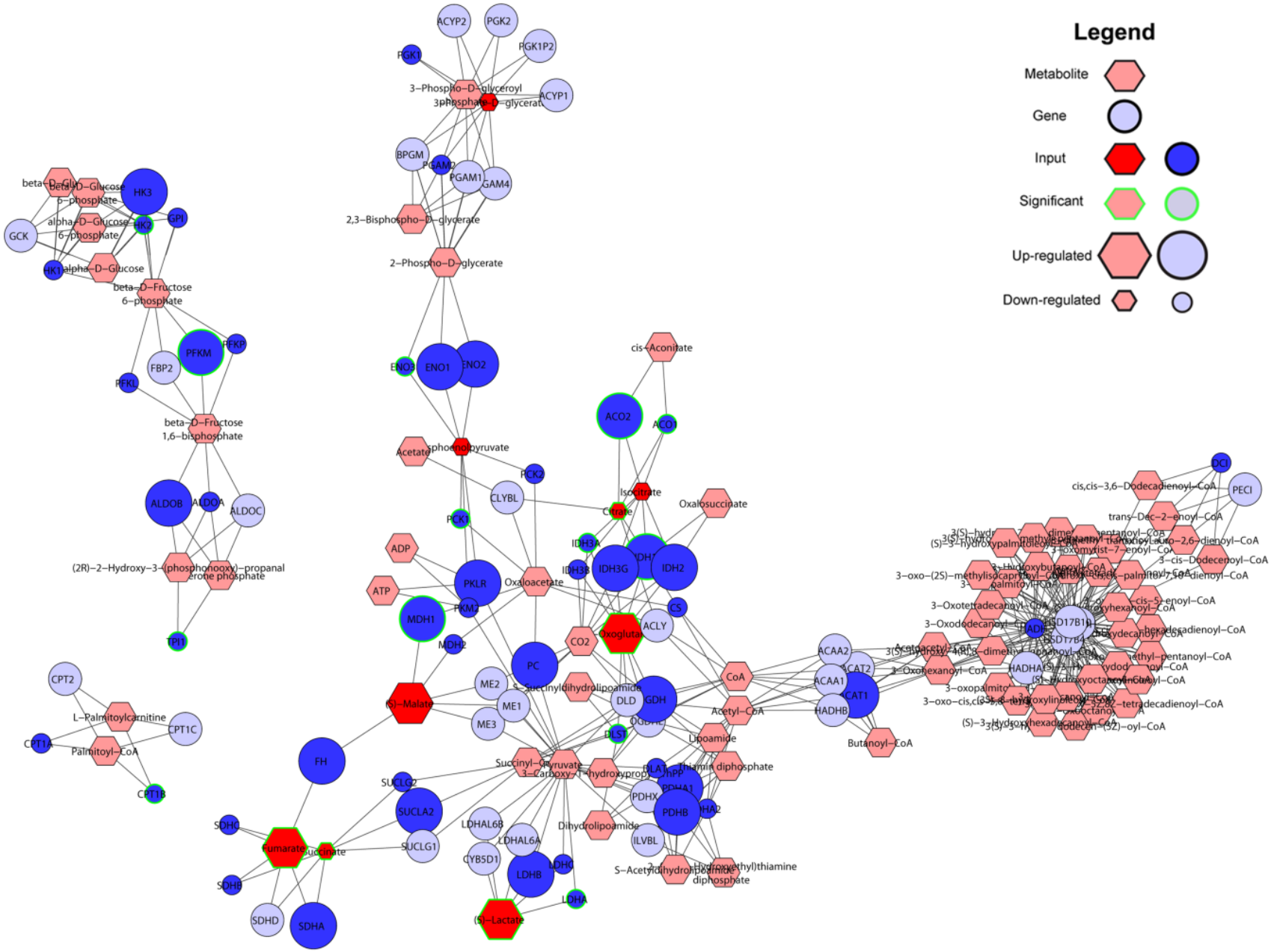

Transcriptomic analysis of kidney tubules from diabetic subjects (Southwestern American Indian cohort, n = 49) compared to non-diabetic healthy living donors (n = 32) along with metabolite data from urine of subset of diabetic subjects (Southwestern American Indian cohort, n = 26) and controls (n = 28) was visualized using CytoScape with the MetScape plugin. A subnetwork containing glycolysis, TCA cycle and pathways involving β-oxidation was generated to focus on the pathways of interest.

Supplemental Figure 7: MetScape analysis of mouse kidney cortex transcriptome and metabolome

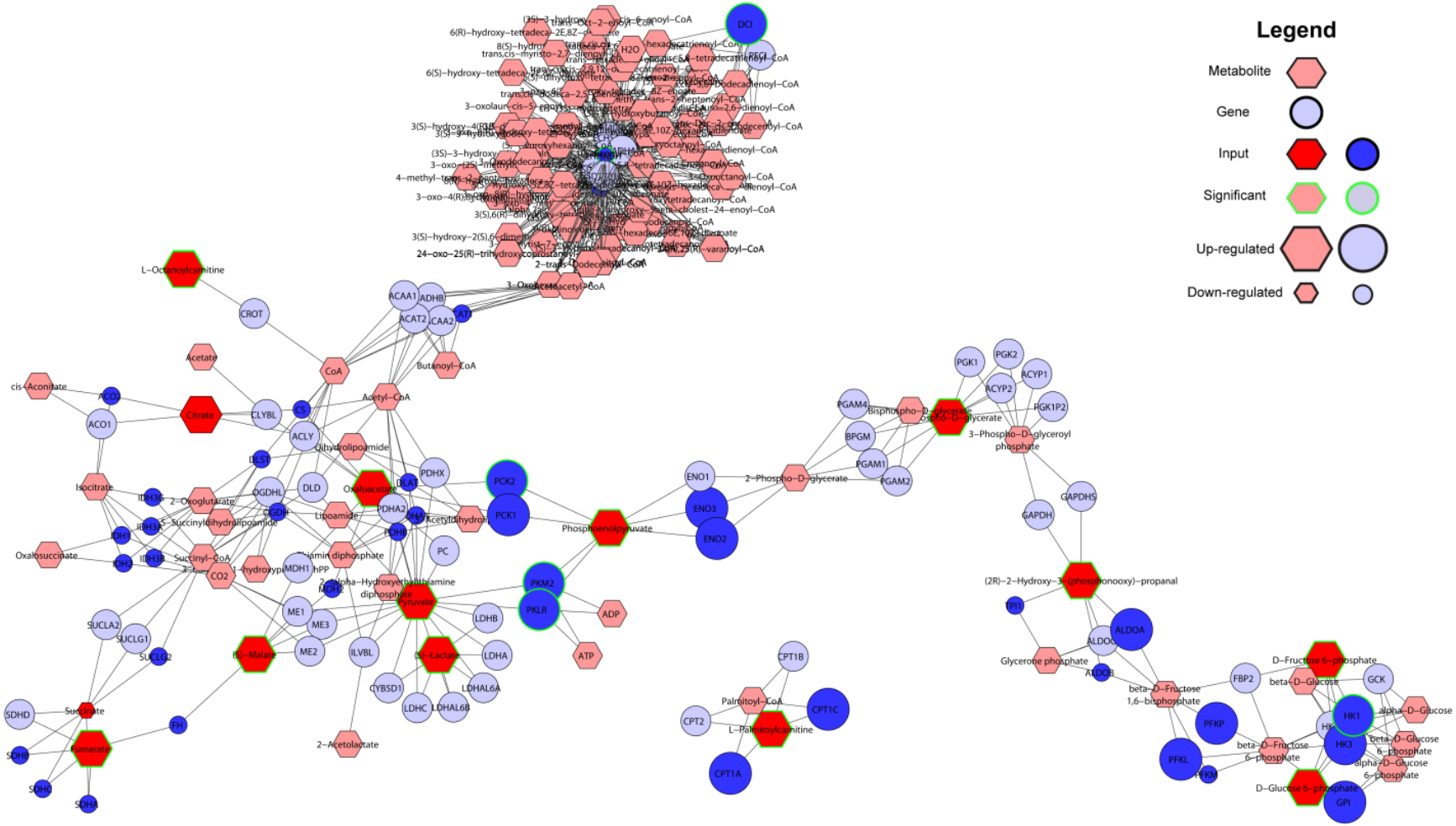

Transcriptomic (n = 5/group) and metabolomics (n = 12/group) data from 24-week-old diabetic versus control mice were analyzed using the visualization tool CytoScape with the MetScape plugin to examine the concordance of results obtained with each method. A subnetwork containing glycolysis, TCA cycle and pathways involving β-oxidation was generated to focus on the pathways of interest.

Supplemental Figure 8: Metabolomic analysis of urine from FinnDiane study participants with and without renin-angiotensin-aldosterone system blockade

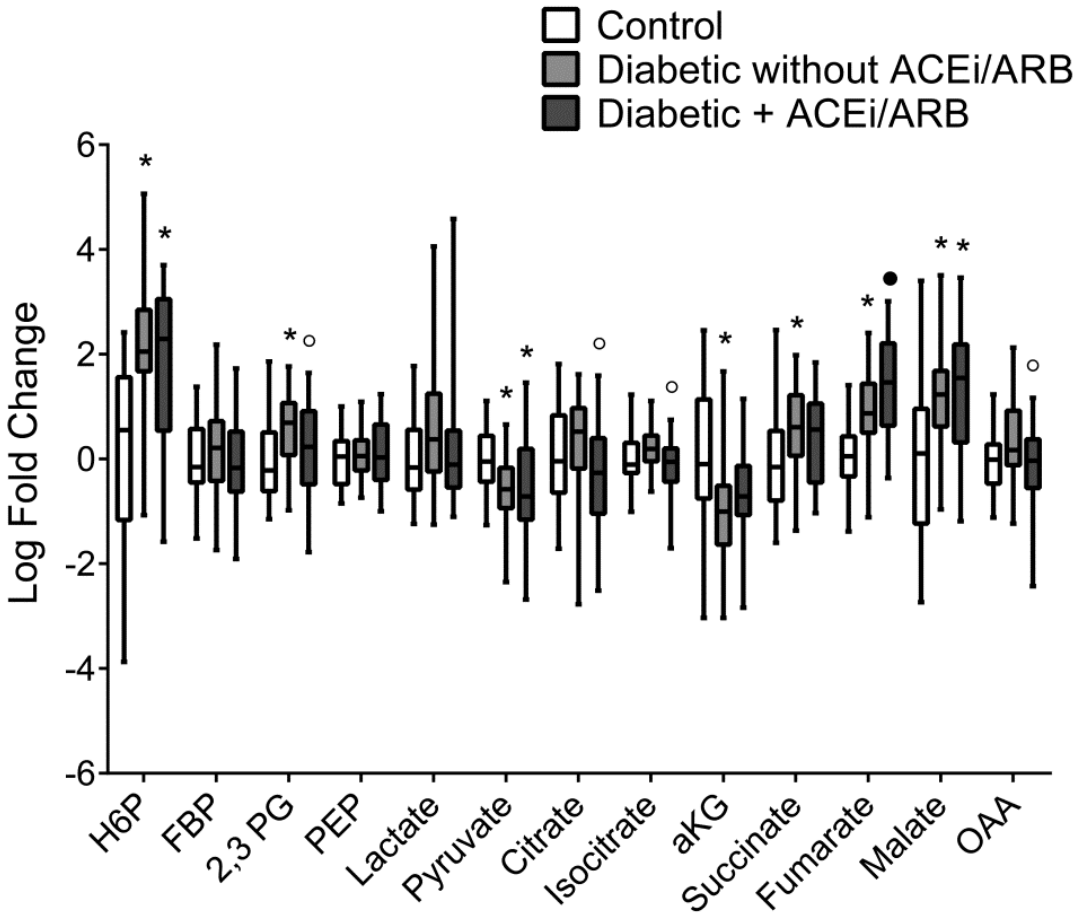

Levels of metabolites in urine from FinnDiane study participants [* $p < 0.05$ versus controls (n = 28), ° $p < 0.05$ versus diabetics without ACEi/ARB, • $p < 0.05$ versus controls and diabetics without ACEi/ARB]. Diabetic patients without ACEi/ARB (n = 38) versus diabetic patients on ACEi or ARB (n = 34) had similar eGFR (mean 90.0 mL/min/1.73m^2 versus 82.0 mL/min/1.73m^2, p = 0.2865, one-way ANOVA with Tukey's multiple comparisons) and UACR (median 6.4 mg/g versus 40.7 mg/g, p = 0.0661, Kruskal-Wallis with Dunn's multiple comparisons). There were no significant differences in age or duration of diabetes between diabetic patients with or without ACEi/ARB.

Supplemental Figure 9: Metabolomic analysis of urine at baseline and follow-up in patients with progressive diabetic kidney disease

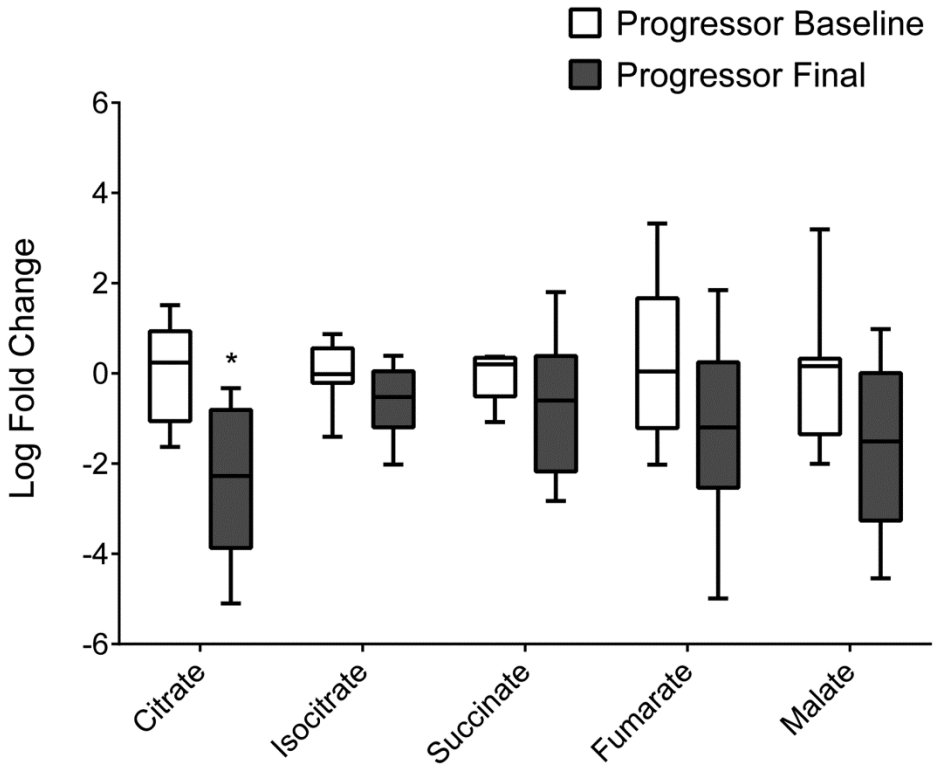

Levels of TCA cycle metabolites in final visit versus baseline urine from diabetic progressor subjects enrolled in the FIND study (n = 9). Median follow-up was 5.56 years (range 2.13 – 7.59). At time of final visit, patients had a median eGFR of 49.0 mL/min/1.73m^2 (range 31.0 – 64.0) and a median UPCR of 55.0 mg/g (range 4.0 – 4240). * $p < 0.05$, student's t-test or Welch's unequal variances t-test.